HHS Public Access

Author manuscript

Anticancer Res. Author manuscript; available in PMC 2015 April 07.

Published in final edited form as:

Anticancer Res. 2014 July ; 34(7): 3293–3302.

Differential Growth Inhibition of Cerebral Metastases by Anti-angiogenic Compounds

DANIEL K. MARTIN[1], **ORTRUD UCKERMANN**[1], **AIKO BERTRAM**[1], **CORINA LIEBNER**[1], **SANDY HENDRUSCHK**[1], **KERIM HAKAN SITOCI-FICICI**[1], **GABRIELE SCHACKERT**[1], **EDITH M. LORD**[3], **ACHIM TEMME**[1,2], and **MATTHIAS KIRSCH**[1,2]

[1]Department of Neurosurgery, Carl Gustav Carus University Hospital, Dresden University of Technology, Dresden, Germany

[2]CRTD/DFG-Center for Regenerative Therapies Dresden, Dresden University of Technology, Dresden, Germany

[3]Department of Microbiology and Immunology, James P. Wilmot Cancer Center, University of Rochester, Rochester, NY, U.S.A

Abstract

Background—The formation of brain metastases is intrinsically linked to concomitant angiogenesis. The purpose of the present study was to investigate the combined effects of interleukin-12 (IL-12) and EMD121974 on the growth and distribution of melanoma brain metastases since both substances may interact with important steps in the cascade of brain metastases formation.

Materials and Methods—Brain metastases were induced by either stereotactic implantation of cells to the brain parenchyma or by injection of the melanoma cells into the internal carotid artery to mimic hematogenous metastatic spread in mice. Naive or IL-12-overexpressing murine K1735 melanoma cells were used either alone or in combination with intraperitoneal anti-integrin treatment using EMD121974.

Results—Solid melanoma metastases were more susceptible to daily low-dose treatment of EMD121974 than multiple hematogenous metastases. Interleukin-12 had a profound effect on both types of brain metastases. After 21 days, a marked reduction of vascularity was observed in both tumor types.

Conclusion—The combination of endogenous IL-12 production with integrin blockade resulted in additive effects for murine hematogenous brain metastases but not for focal brain metastases.

Keywords

Brain metastases; melanoma; interleukin-12; EMD121974; cilengitide; brain tumor

Correspondence to: Prof. Dr. med. Matthias Kirsch, Klinik und Poliklinik für Neurochirurgie, Carl Gustav Carus Universitätsklinikum an der Technischen Universität Dresden, Fetscherstrasse 74, D-01307 Dresden, Germany. Tel: +493514584735, Fax: +49 3514584304, matthias.kirsch@uniklinikum-dresden.de.

The authors have no competing financial interests.

Brain metastases are the most common brain tumors in adults. Improved treatment of the extra-cerebral primary tumor results in longer survival times and contribute to an increased incidence of brain metastases during the last years. At the time of diagnosis, most patients already have multiple brain metastases, which is associated with an extremely poor prognosis with a median survival of only a few months (10, 12, 20). Lung, breast, and renal carcinomas as well as malignant melanoma belong to a category of tumors with a high tendency to cause brain metastasis. Out of these, malignant melanomas have the highest propensity to metastasize to the brain (18). Formation of brain metastases occurs after the spreading of tumor cells from the primary tumor *via* blood circulation into the brain.

Angiogenesis is a crucial step in tumor development, especially for metastases formation (43). It is a tightly regulated process controlled by the balance of pro- and anti-angiogenic factors (27). In tumors, this physiological balance is disturbed. Hypoxic conditions within the tumor mass may lead to HIF-1α (Hypoxia-inducible factor 1α) upregulation and transcription of pro-angiogenic factors, the most prominent being VEGF (Vascular endothelial growth factor) (8). The metastatic process involves many steps, including intravasation of cells, survival in the blood stream, endothelial attachment in the target organ, extravasation, initial avascular growth, then concomitant angiogenesis, which in itself is a complicated process involving degradation of the vessel basement membrane and extracellular matrix (ECM), migration of endothelial cells and formation of new blood vessels (39). Finally, new, but often disorganized, blood vessels are formed that supply the tumor with oxygen and nutrients (24). The switch of tumor cells into an angiogenic phenotype is one of the decisive steps in early tumor development that gives way to further growth and clinical manifestation of solid tumors. Tumor cells that lack angiogenic activity can stay in a dormant state without causing clinical disease (27, 36). This phenomenon of tumor dormancy emphasizes the importance of angiogenesis in tumor growth (26, 37).

Several factors have been shown to interfere with any of the aforementioned steps in metastases or angiogenesis (1, 26). During angiogenesis, the interaction between the extracellular matrix (ECM) and endothelial cells plays a central role in the adhesion of cells, degradation of the existing vessel network, as well as the migration and spread of endothelial cells. Integrins are the principal transmembrane receptors mediating the adhesion of cells to the ECM (15). Integrin $\alpha_v\beta_3$ is expressed on various cells, such as endothelial cells, fibroblasts, epithelial cells, and smooth muscle cells as well as in many tumors, including melanoma, glioma, breast cancer, and prostate cancer (15). Integrin $\alpha_v\beta_3$ binds specific matrix ligands, such as fibronectin, vitronectin and tenascin-C in gliomas (42).

In a pre-clinical melanoma metastasis model, Mitjans *et al.* demonstrated that inhibition of $\alpha_v\beta_3$ integrins by a specific antibody resulted in a robust treatment response and improvement of survival (34).

EMD 121974, a selective integrin $\alpha_v\beta_3$ antagonist (13), influences multiple aspects of angiogenesis *via* inhibition of the interaction between integrins and their ECM ligands. The compound causes cellular detachment of endothelial and tumor cells (42). It increases apoptosis while decreasing proliferation in both endothelial and glioma cells *in vitro* (38). It was shown to suppress the orthotopic brain tumor growth, promote apoptosis of tumor cells,

and inhibit angiogenesis in nude mice with injected human glioblastoma (U87MG cell line) (33, 45), or medulloblastoma (DAOY cell line) (20) in the forebrain, whereas the heterotopic (subcutaneous) tumor growth was not affected. Therefore, utilization of EMD121974 seems to be of particular interest for cerebral tumors. Recently, it was shown to reduce breast cancer cell migration, invasion, proliferation, and osteoclastic bone resorption in a nude rat model (4, 9). EMD 121974 has undergone clinical trials in patients with recurrent or newly-diagnosed glioblastoma multiforme (GBM).

IL-12 is a heterodimeric immunoregulatory (35-kDa p35 and 40-kDa p40 subunits) cytokine that plays an important role in linking the innate and cell-mediated adaptive immunities to each other. Its principal sources are activated dendritic cells and macrophages. It induces proliferation, activation, and differentiation of type 1 T-helper, NK-cells, and cytotoxic T lymphocytes (CTL) triggering the production of INF-γ by these cells (14, 44, 46). It was shown to exert antitumor activity in murine tumor models of glioma, breast cancer, melanoma, colon, and renal carcinoma (16, 22), as well as in human neoplastic cells from hematopoietic and bronchial malignancies (17). IL-12 modulates tumor genetic program *via* INF-γ-dependent induced genes (2) and INF-γ-independent induced genes (41), altering the expression of pro-angiogenic and anti-angiogenic molecules. This way, the downstream effects of IL-12 resulted in inhibition of angiogenesis and remodeling of the extracellular matrix and induction of chemokines. IL-12-modulated immune system exerts antitumor activity and so IL-12 induces this protective immunity against all tumor cell lines (*i.e.* K1735 melanoma cells) (35). IL-12 has also been investigated in clinical phase I/II studies, mostly in combination with other agents, in a variety of tumors; the majority of them being malignant melanoma, renal cell carcinoma, and lymphomas. The exerted clinical efficacy ranged between minimal response (3, 31), stable disease (5, 30), and modest tumor regression (11, 23). However, most glioma patients have a suppressed local immune response. Therefore, the non-immunological effects of IL-12 might suffice for an antitumor response.

The purpose of the present study was to investigate the combined effects of IL-12 and EMD121974 on growth and distribution of melanoma brain metastases since both substances may interact with important steps in the cascade of brain metastases formation.

Materials and Methods

Cell lines

The murine melanoma cell line K1735 (kindly provided by Margaret Kripke and Isaiah Fidler, M.D. Anderson Cancer Center, Houston, Texas, USA) (29) and K1735 transfected with murine IL-12 (kindly provided by Edith M. Lord, Wilmot Cancer Center, University of Rochester, Rochester, NY^{50}) were used for the induction of brain metastases.

Cells were grown as monolayers in Dulbecco's modified Eagle's medium (Gibco, Grand Island, NY, USA), supplemented with 300 ng/ml L-glutamine, 10 mM Hepes (Biochrom/ Seromed KG, Berlin, Germany) and 10% fetal bovine serum. Cultures were maintained at 37°C in 5% CO_2 and 95% air in a humidified atmosphere.

Animals

All animal experiments were conducted in accordance with the guidelines of the Technical University in Dresden, Germany, based on National laws and are in full agreement with the European Union directive on animal experimentation. Experiments were performed on female nude mice NMRI$^{nu/nu}$ aged six to eight weeks.

These studies were performed in nude mice to focus on the anti-angiogenic effects of the treatments separately from any immunological effects. Animals were kept under pathogen-free conditions and received food and water *ad libitum*.

Induction of brain metastases

All mice were anesthetized by intra-peritoneal injection of ketamine/xylazine. Brain metastases were induced either as focal singular tumors *via* stereotactic implantation of melanoma cells into the brain parenchyma of the right frontal lobe (STX group), or were induced as diffuse one-sided metastases *via* injection of melanoma cells into the internal carotid artery (ICA group) to simulate hematogenous metastatic spread.

Stereotactic injection

After midline scalp incision, a burr hole was made using a dental drill. Tumor cells (10^3 cells in 5 μl PBS) were injected slowly into the right frontal lobe using a stereotactic device (Stoelting, Wood Dale, IL, USA) equipped with a Hamilton syringe. The burr hole was closed with bone wax and the incision was sutured with 7-0 silk.

Injection into the internal carotid artery

Hematogenous brain metastases were experimentally induced by injection of tumor cells into the internal carotid artery of the mice, as previously described (40). The right common carotid artery was prepared using a dissecting microscope. After nicking the artery with a pair of microscissors, a glass cannula was inserted into the lumen and threaded forward into the internal carotid artery. After slow injection of 100,000 cells in 100 μl PBS, the cannula was removed, the artery ligated with 5-0 silk and the skin was closed as described above.

Treatment with EMD121974

Three days after tumor induction, the mice received daily intraperitoneal 100 mg EMD121974 (EMD121974, MERCK KGaA, Darmstadt, Germany) injections for a total of 7 days. The control group received injections of 0.9 % NaCl.

Experimental end-points

To evaluate the impact of EMD121974 treatment and IL-12 expression on survival, mice were euthanized when reaching a defined end-point: occurrence of neurological deficits or bodyweight reduction of more than 25 %. For histological analysis of brain and of tumor tissue progression, a second set of animals of all experimental groups were euthanized 16 days after injection of melanoma cells.

Tissue processing

Animals were euthanized by injection of an overdose of pentobarbital. After removal of the brain, the tissue was embedded in tissue-freezing medium (Leica, Nussloch, Germany), snap-frozen on dry ice, and stored at −80°C. Subsequently, sections of 10 μm thickness were prepared, fixed in methanol-acetone (1:1), and stored at −20°C until use. Prior to further processing, sections were allowed to thaw for 30 min. To confirm the successful formation and the localization of brain metastases, sections were stained with hematoxylin and eosin. Sections were washed in distilled water and incubated in Meyer's hematoxylin/hemalaun for 3 min. After washing again, the tissue was briefly destained in HCl-ethanol. Washing using tap water for 5 min was followed by 3 min staining in eosin (1% eosin G in 80% ethanol). The sections were dehydrated with rising ethanol concentrations, cleared in xylene, and coverslipped using DePeX mounting medium (SERVA Electrophoresis GmbH, Heidelberg, Germany).

For immunohistochemistry, the sections were blocked with 0.1 % bovine serum albumin and 3% normal goat serum in 0.3 % TritonX for 1 h and probed with the primary antibody for 1 h. After washing with PBS, sections were incubated with the secondary antibody followed by colorimetric detection of the antibody signal. In detail, the following antibodies and detection kits were used: anti-CD31 (1:500, kindly provided by Prof. Georg Breier, Department of Pathology, Universitätsklinikum Dresden) was detected using Vectastain Elite ABC Kit Rat IgG (Vector Laboratories Inc., Burlingame, CA, USA) followed by AEC-kit. The sections were counterstained with eosin and coverslipped with Aquatex (MERCK KGaA, Darmstadt, Germany). Anti-Ki67 (1:500, Novocastra, Leica Microsystems, Wetzlar, Germany) was used with prior heat antigen retrieval in citrate buffer and in combination with histofine simple stain MAX Po (Nicheirei Biosciences Inc., Tokyo, Japan) followed by histogreen detection, counterstaining with nuclear fast red and mounted with DePeX.

To detect apoptotic cells, TUNEL (TdT mediated dUTP nick end labeling) staining of brain sections was carried out using the ApopTagRed *in situ* Apoptosis Detection Kit (Chemicon International, Deutschland, Hofheim am Taunus, Germany) according to the manufacturer's instructions. Slides were allowed to briefly thaw and then were postfixed with 1% PFA (pH 7.4) for 1 h at room temperature. Washing with PBS was followed with ethanol/acetic acid (2:1) for 5 min at −20°C and then the sections were rinsed again with PBS. After incubation in equilibration buffer for 10 sec, the TDT enzyme was applied for 1 h at 37°C. The reaction was stopped using the working strength stop/wash buffer for 10 min. The TUNEL-signal was visualized using anti-dioxigenin-rhodamine for 30 min. The specimens were coverslipped using Vectashield (Vector Laboratories, Burlingame, USA) with DAPI nuclear counterstaining.

Qunatification of microvessels, proliferation and apoptosis

Microvessel density was measured under light microscopy at 200-fold magnification in a single area of invasive tumor representative of the highest microvessel density (28, 32). Every positive-staining endothelial cell or cell cluster that was separate from other microvessels was counted. The presence of a vascular lumen was not necessary to identify a microvessel. Glomeruloid clusters were counted as one microvessel.

The potential impact of treatment on angiogenesis was evaluated by analyzing microvessel densities within the brain metastasis as well as in normal brain tissue according to (28). Therefore, all CD31 positive structures in one field of view were counted at 200-fold magnification. Additionally, the morphology of microvessels was evaluated in a blinded fashion. The appearance of the structures (very fine, fine, coarse) as well as the pattern of the vessels (regular or irregular) was analyzed and transformed to a scoring system (vascular index: 0=very fine, regular; 1=fine, regular; 2=coarse, regular; 3=coarse, irregular).

For *in situ* detection of apoptosis, slides were incubated with 20 mg/ml proteinase K for 15 min at room temperature and quenched in 2 % hydrogen peroxide in PBS for 5 min. Apoptosis was detected by the TUNEL-method using the Apotag Kit (Oncor, Gaithersburg, MD) followed by counterstaining with nuclear fast red (Vectorlabs, Peterborough, UK). Sections of post-partum rat mammary gland (Oncor) served as positive control, and slides where terminal transferase was omitted served as negative control. The apoptotic index was defined as the percentage of positively stained cells per 100 nuclei from 10 randomly chosen fields per section, scored under light microscopy at 200-fold magnification. Proliferation was calculated accordingly using a specific anti-Ki67 nuclear antigen antibody. In addition, standard hematoxylin/eosin staining of each tumor specimen was also performed.

Statistical analysis

All data are expressed as mean±SD. Statistical analysis (*t*-test or ANOVA followed by Tukey Multiple Comparison test, Log-rank test for survival data) was performed using Graph Pad Prism 5.0 (Graph Pad Software Inc., La Jolla, CA, USA). The number of animals in the experimental groups was n=5–8 unless stated otherwise.

Results

Brain metastases were induced in nude mice either by stereotactic implantation (STX) or intracarotid injection (ICA) of melanoma cells. We investigated the impact of anti-angiogenic therapies using internal expression of IL-12 (K1735-IL12 cells), systemic EMD121974 treatment, or a combination of both therapies on tumor development.

Survival

Focal single melanomas induced *via* stereotactic intracranial injection (STX) of wtK1735 melanoma cells had a median survival time of 21.5 ±2 days without therapy (Figure 1A). The different treatment modalities; endogenous IL-12 expression, EMD121974 administration, or the combination of both resulted in a significant increase of the median survival times (30, 29 and 31.5 days, respectively, $p<0.001$). There were no differences concerning the survival times among the treatment groups. In particular, the combination of endogenous IL-12 expression did not result in longer survival if combined with integrin receptor blockade by EMD121974.

In the hematogenous metastasis model (ICA), both EMD121974 treatment and IL-12 expression resulted in a significant increase in survival, with IL-12 expression being more effective than EMD121974 ($p<0.05$ and $p<0.001$, respectively; Figure 1B). The combination resulted in additive effectiveness ($p<0.001$). The integrin inhibitor alone exhibited only a

moderate effect on survival time (median survival: control=22 days; EMD121974=26 days), whereas the endogenous expression of IL-12 resulted in a considerably prolonged survival in this model (IL-12=33 days). The additional blockade of the integrin receptors slightly enhanced the IL-12 effect (IL-12 + EMD121974=36 days).

Metastases formation

Anti-angiogenic therapy led to different response rates in the focal (STX) *versus* hematogenous (ICA) brain metastasis models. In particular, EMD121974 had a strong effect in the STX model but only moderate impact on survival in the ICA group. The impact of therapies on tumor properties, namely vascularization, proliferation, and apoptosis was investigated by histology 16 days after tumor induction. This time point was chosen to monitor early effects before animals in the control group began to exhibit signs of solid tumor growth. Brain tissue of animals in the STX treatment groups was additionally investigated at a late stage of tumor growth for those animals that had to be euthanized. Stereotactic implantation of wt-K1735 cells resulted in formation of localized solid tumors surrounded by clusters of spreading metastases (Figure 2A and 4A) and was described previously in a different set of experiments (28). Tumor formation was accompanied by mild to massive changes in the pattern of blood vessels that were investigated by CD31 staining (Figure 2A).

Hematogenous metastases of the ICA group revealed alterations of the microvessel pattern and proliferation index (Figure 2A and 4A). After 16 days, we detected clusters of tumor cells of various sizes in multiple brain regions in all animals. These were accompanied by clear but moderate changes in microvessel architecture and clusters of Ki67-positive cells. Additionally, we found single Ki67-positive cells distributed among the ipsilateral brain parenchyma, probably indicating the latent metastases.

Vascularity

Tumor formation led to obvious changes in the microvessel architecture indicated by altered CD31 staining patterns. Within brain metastases, the appearance of microvessels was gradually transformed from a very fine and regular pattern (vascular index=0) towards a coarse and irregular morphology (vascular index=3) (Figure 2A). Vascularity including microvessel morphology was categorized, showing that in all treatment groups, the tumor-induced vascularity changes were shifted to a more normal, *e.g.*, finer and more regular phenotype.

At 16 days post-implantation, all solid intra-cranial tumors displayed a coarse vessel morphology in a regular or even irregular pattern (Figure 2B). The mean vascular index in all treatment groups was significantly lower for animals that had received mk1735-IL-12 cells. In 40% of animals with a combination of EMD121974 and IL-12 therapy, we found no vascular alterations at all. We did not find an irregular vascular pattern in any of the treated animals. In long surviving prefinal animals, blood vessel architecture was notably changed in all treatment groups and resembled 16-day-old-untreated tumors (Figure 2A).

In the hematogenous metastases model, the evaluation of CD31-positive microvessels revealed a fine to coarse phenotype compared to very fine structures in normal tissue (Figure 2A and 2C). In contrast to the STX-model, the pattern of vessels in all animals without therapy was regular and some displayed a fine vasculature (Figure 2A). We found no marked differences in the overall morphology of CD31-positive structures in metastases between control animals and animals of the treatment groups, although there might have been a trend towards a finer microvessel appearance in tumors of treated animals. In long-surviving prefinal animals with hematogenous metastases, the microvessel architecture was dramatically changed in all experimental groups towards a coarse and irregular phenotype (Figure 2A).

Comparing the microvessel index of animals of the different metastases models, a coarse and irregular microvessel structure was developed at a later time point after tumor induction in the ICA-model. The application of anti-angiogenic drugs only had an impact on microvessel phenotype in the STX-model: The different therapies slowed-down the development of an abnormal microvessel network to a similar extent, but were not able to prevent tumor induced changes.

Microvessel density

Microvessel densities (MVD) were up to 40% lower in tumors of all treatment groups compared to the contralateral normal brain tissue (Figure 3). This is consistent with former findings (7). 16 days after stereotactic implantation of K1735 cells (STX) of the control group revealed a substantial reduction of microvessel density. All anti-angiogenic therapies had higher microvessel densities than control tumors; however, we only found significant differences in the combined-treatment group (Figure 3A). At the median survival time (24 days) the number of CD31-positive structures in the EMD121974 and IL-12 groups was comparable to controls. Surprisingly, the combination of IL-12 and EMD121974 was more effective in preventing tumor-induced reduction of microvessel density in these late-stage tumors. The microvessel density was significantly higher in this experimental group and was equal to that at 16 days of survival.

After metastasis induction by intracarotid injections, the density of microvessels of late-stage tumors was strongly reduced by more than 40% compared to normal brain tissue (Figure 3B, dotted line). This is comparable with the reduction seen in untreated animals in the STX-model after 16 days of survival. Neither anti-angiogenic therapy nor survival time changed the microvessel density observed in the hematogenous metastases model.

Proliferation

The degree of proliferation was analyzed by estimating the proportion of Ki67-positive cells in the melanoma metastasis. After stereotactic implantation, a considerable number of proliferating cells was observed within the brain tumors. Analysis of the number of Ki67-positive nuclei at 16 days of survival revealed a clear reduction of proliferation after anti-angiogenic therapy (Figure 4A). Again, this effect of treatment was only transient. Late-stage tumors revealed significantly increased proliferation in all treatment arms, which was

comparable to untreated controls. There were no differences within the three therapy groups, EMD121974, endogenous IL-12 expression, or a combination of both.

In the hematogenous metastasis model, there were fewer proliferating cells in the tumor areas than in the STX model in the control group (Figure 4B). This low proliferation remained constant even at longer survival times. In contrast to the findings in metastases induced by intra-cranial injection of melanoma cells, none of the anti-angiogenic therapies influenced the proliferation rate seen in the ICA-metastases model.

Apoptosis

TUNEL-staining provided information on apoptosis, but only a few apoptotic cells were detected even in larger tumors in both metastases models. No significant difference among the treatment arms was found, although apoptotic cells were rarely found in animals receiving anti-angiogenic therapy (data not shown).

Discussion

We have shown that both EMD and IL-12 independently had a significant therapeutic benefit on the progression of experimental melanoma brain metastases regardless of the type of tumor induction. However, we did not observe a synergistic treatment effect. An additive benefit was only observed for hematogenous brain metastases. We investigated two different models to induce brain metastases which differ in the complexity of the metastatic process. The two models were either i) direct introduction of tumor cells by stereotactic injection into the target tissue or ii) intra-arterial injection into the brain supplying carotid artery. The latter technique required tumor cells to complete steps along the metastatic cascade, including but not limited to endothelial adherence, basal membrane infiltration, extravasation, and migration. It is interesting that focal tumors have a different growth pattern compared to hematogenous metastases. Usually, solid metastases develop after injection of tumor cells into the brain parenchyma. They develop a classical type of tumor-angiogenesis and show central necrosis at late stages (28).

In contrast, intra-arterial injection results in disseminated hematogenous BM, which have an initial perivascular cuffing-type growth pattern. Only at later stages does classical angiogenesis begin (6). For these reasons, we expected to observe differences in response to local and systemic therapies in growth pattern and early angiogenesis. This would be of importance since the hematogenous metastases model mimics the clinical metastatic process more closely.

The systemic treatment of EMD for one week had a significant effect on survival for direct intra-cerebral injection of melanoma cells but not for hematogenous metastases. Hematogenous metastases were treated for one week starting on post-injection day 3, which might have ignored early steps of the metastatic process. Although this might be counterintuitive on a biological level, the clinical situation is equivalent; patients are usually treated with the notion that micrometastases exist, *e.g.* after surgical removal of a single solid metastasis. Immediately after EMD single or combined treatment on day 16 in single BM (STX group), proliferation was suppressed but recovered until the prefinal stage in

single BM, whereas no difference occurred in hematogenous multiple BM at different stages of development. Therefore, the effect on proliferation was more likely to be independent of any treatment arm in focal and hematogenous BM. Overall, hematogenous BM had a lower proliferation index, which is due to the infiltrative perivascular growth pattern of these metastases resulting in a relatively higher normal parenchyma contamination during counting of Ki67+ nuclei.

The effects on vascularity were modest in the hematogenous model: the early vascularization was low, which is most likely due to the initial perivascular growth pattern. At late stages, neovascularization ensued and resulted in high vascularity indexes for all treatment arms. For focal tumors, all treatment arms resulted in inhibition of vascularity at early stages compared to controls. However, at late stages, tumor growth recovered and vascularity was equal to controls. The difference in treatment response at 16 days – early after treatment – suggests a vascularization specific effect of both EMD and IL-12, which was ablated upon recovery and tumor progression.

We tested endogenous overexpression of IL-12 as an additional anti-angiogenic factor and were able to verify earlier observations by Moran *et al.* (31) that IL-12 is a potent inhibitor of melanoma metastases growth. Moran *et al.* reported that tumors remained in a dormant state for 3–4 weeks until IL-12-negative tumor cells were responsible for tumor recurrence (31). We recorded tumor growth upon histological examination for all animals within 16 days. In our series, IL-12 significantly inhibited tumor growth for both focal (STX) and disseminated (ICA) brain metastases.

For all treatment arms, vascularity was reduced with a more permanent effect on solid STX tumors rather than disseminated ICA tumors. In contrast, the antitumor effect was more pronounced in the ICA compared to the STX group. Therefore, classical angiogenesis might be the preferred target compared to perivascular cuffing. Our results do not indicate which of the therapeutic compounds are responsible for the preferential effects on angiogenesis type and tumor growth in the two different tumor initiation models.

IL-12 has been studied for metastatic melanoma in two phase I trials and is currently being investigated in more than 40 clinical trials for various tumor types (clinicaltrials.gov). However, as of now there is no standard treatment regime including IL-12.

The effect of EMD 121974 on other cancers and metastases was somewhat less promising. EMD 121974 has been under clinical investigation in a phase II clinical trial for metastatic melanoma (25) and advanced solid tumors (21) in which single-agent EMD 121974 treatment showed good tolerance to the drug and minor partial clinical responses with only minimal clinical efficacy. EMD 121974 as a single agent did not cause tumor regression, despite the post-treatment increases in tumor and endothelial cell apoptosis (21). A multi-national phase II clinical trial comparing EMD 121974 plus gemcitabine against gemcitabine alone in unresectable pancreatic cancer showed a median overall survival of 6.7 months in the EMD 121974 plus gemcitabine group and 7.7 months in the gemcitabine-alone group with median progression free survival of 3.6 months and 3.8 months, respectively (19). Currently, more than 11 trials have been announced which are using

EMD1212974 for brain tumors or metastatic melanoma and one ongoing phase II clinical trial for recurrent glioma (Glarius-study) is running (clinicaltrials.gov).

In summary, endogenous IL-12 expression in melanoma cells and integrin blockade significantly inhibited melanoma brain metastasis. The combination of both therapies did not result in an additive or synergistic effect for focal tumors, but additive effects for hematogenous metastases, indicating that the metastatic cascade is altered in addition to local anti-angiogenic effects.

Acknowledgments

We would like to thank Felicitas Zachow and Elke Leipnitz for excellent technical support, Dr. Fidler for supplying the K1735 cell line, and the Animal Facility crew for their continuous support and animal care. EMD121974 (Cilengitide) was kindly provided by MERCK KGaA, Darmstadt, Germany.

References

1. Airoldi I, Di Carlo E, Cocco C, Taverniti G, D'Antuono T, Ognio E, Watanabe M, Ribatti D, Pistoia V. Endogenous IL-12 triggers an antiangiogenic program in melanoma cells. Proceedings of the National Academy of Sciences of the United States of America. 2007; 104:3996–4001. [PubMed: 17360466]
2. Airoldi I, Ribatti D. Regulation of angiostatic chemokines driven by IL-12 and IL-27 in human tumors. Journal of leukocyte biology. 2011; 90:875–882. [PubMed: 21750124]
3. Anwer K, Barnes MN, Fewell J, Lewis DH, Alvarez RD. Phase-I clinical trial of IL-12 plasmid/lipopolymer complexes for the treatment of recurrent ovarian cancer. Gene therapy. 2010; 17:360–369. [PubMed: 20033066]
4. Bauerle T, Komljenovic D, Merz M, Berger MR, Goodman SL, Semmler W. Cilengitide inhibits progression of experimental breast cancer bone metastases as imaged noninvasively using VCT, MRI and DCE-MRI in a longitudinal *in vivo* study. International journal of cancer Journal international du cancer. 2011; 128:2453–2462. [PubMed: 20648558]
5. Bekaii-Saab TS, Roda JM, Guenterberg KD, Ramaswamy B, Young DC, Ferketich AK, Lamb TA, Grever MR, Shapiro CL, Carson WE 3rd. A phase I trial of paclitaxel and trastuzumab in combination with interleukin-12 in patients with HER2/neu-expressing malignancies. Molecular cancer therapeutics. 2009; 8:2983–2991. [PubMed: 19887543]
6. Bergers GBL. Tumorigenesis and the angiogenic switch. Nat Rev Cancer. 2003; 3:401–410. [PubMed: 12778130]
7. Brahimi-Horn C, Berra E, Pouyssegur J. Hypoxia: the tumor's gateway to progression along the angiogenic pathway. Trends in cell biology. 2001; 11:S32–36. [PubMed: 11684440]
8. Brahimi-Horn MC, Bellot G, Pouyssegur J. Hypoxia and energetic tumour metabolism. Current opinion in genetics & development. 2011; 21:67–72. [PubMed: 21074987]
9. Bretschi M, Merz M, Komljenovic D, Berger MR, Semmler W, Bauerle T. Cilengitide inhibits metastatic bone colonization in a nude rat model. Oncology reports. 2011; 26:843–851. [PubMed: 21725616]
10. Caroli M, Di Cristofori A, Lucarella F, Raneri FA, Portaluri F, Gaini SM. Surgical brain metastases: management and outcome related to prognostic indexes: a critical review of a ten-year series. ISRN surgery. 2011; 2011:207103. [PubMed: 22084749]
11. Daud AI, DeConti RC, Andrews S, Urbas P, Riker AI, Sondak VK, Munster PN, Sullivan DM, Ugen KE, Messina JL, Heller R. Phase I trial of interleukin-12 plasmid electroporation in patients with metastatic melanoma. Journal of clinical oncology: official journal of the American Society of Clinical Oncology. 2008; 26:5896–5903. [PubMed: 19029422]
12. DeAngelis LM. Brain tumors. The New England journal of medicine. 2001; 344:114–123. [PubMed: 11150363]

13. Dechantsreiter MA, Planker E, Matha B, Lohof E, Holzemann G, Jonczyk A, Goodman SL, Kessler H. N-Methylated cyclic RGD peptides as highly active and selective alpha(V)beta(3) integrin antagonists. Journal of medicinal chemistry. 1999; 42:3033–3040. [PubMed: 10447947]
14. Del Vecchio M, Bajetta E, Canova S, Lotze MT, Wesa A, Parmiani G, Anichini A. Interleukin-12: biological properties and clinical application. Clinical cancer research: an official journal of the American Association for Cancer Research. 2007; 13:4677–4685. [PubMed: 17699845]
15. Desgrosellier JS, Cheresh DA. Integrins in cancer: biological implications and therapeutic opportunities. Nature reviews Cancer. 2010; 10:9–22.
16. Dias S, Boyd R, Balkwill F. IL-12 regulates VEGF and MMPs in a murine breast cancer model. International journal of cancer Journal international du cancer. 1998; 78:361–365. [PubMed: 9766572]
17. Ferretti E, Di Carlo E, Cocco C, Ribatti D, Sorrentino C, Ognio E, Montagna D, Pistoia V, Airoldi I. Direct inhibition of human acute myeloid leukemia cell growth by IL-12. Immunology letters. 2010; 133:99–105. [PubMed: 20705102]
18. Flanigan JC, Jilaveanu LB, Chiang VL, Kluger HM. Advances in therapy for melanoma brain metastases. Clin Dermatol. 2013; 31:264–281. [PubMed: 23608446]
19. Friess H, Langrehr JM, Oettle H, Raedle J, Niedergethmann M, Dittrich C, Hossfeld DK, Stoger H, Neyns B, Herzog P, Piedbois P, Dobrowolski F, Scheithauer W, Hawkins R, Katz F, Balcke P, Vermorken J, van Belle S, Davidson N, Esteve AA, Castellano D, Kleeff J, Tempia-Caliera AA, Kovar A, Nippgen J. A randomized multi-center phase II trial of the angiogenesis inhibitor Cilengitide (EMD 121974) and gemcitabine compared with gemcitabine alone in advanced unresectable pancreatic cancer. BMC cancer. 2006; 6:285. [PubMed: 17156477]
20. Gavrilovic IT, Posner JB. Brain metastases: epidemiology and pathophysiology. Journal of neuro-oncology. 2005; 75:5–14. [PubMed: 16215811]
21. Hariharan S, Gustafson D, Holden S, McConkey D, Davis D, Morrow M, Basche M, Gore L, Zang C, O'Bryant CL, Baron A, Gallemann D, Colevas D, Eckhardt SG. Assessment of the biological and pharmacological effects of the alpha nu beta3 and alpha nu beta5 integrin receptor antagonist, cilengitide (EMD 121974), in patients with advanced solid tumors. Annals of oncology: official journal of the European Society for Medical Oncology/ESMO. 2007; 18:1400–1407. [PubMed: 17693653]
22. Hong X, Miller C, Savant-Bhonsale S, Kalkanis SN. Antitumor treatment using interleukin- 12-secreting marrow stromal cells in an invasive glioma model. Neurosurgery. 2009; 64:1139–1146. discussion 1146-1137. [PubMed: 19487894]
23. Kikuchi T, Akasaki Y, Abe T, Fukuda T, Saotome H, Ryan JL, Kufe DW, Ohno T. Vaccination of glioma patients with fusions of dendritic and glioma cells and recombinant human interleukin 12. Journal of immunotherapy (Hagerstown, Md: 1997). 2004; 27:452–459.
24. Kim K-W. Brain angiogenesis in developmental and pathological processes. The FEBS journal. 2009; 276:4621. [PubMed: 19664073]
25. Kim KB, Prieto V, Joseph RW, Diwan AH, Gallick GE, Papadopoulos NE, Bedikian AY, Camacho LH, Hwu P, Ng CS, Wei W, Johnson MM, Wittemer SM, Vardeleon A, Reckeweg A, Colevas AD. A randomized phase II study of cilengitide (EMD 121974) in patients with metastatic melanoma. Melanoma research. 2012; 22:294–301. [PubMed: 22668797]
26. Kirsch M, Allende R, Black P, Schackert G. Endogenous growth inhibition of angiogenesis in brain tumors. Cancer metastasis reviews. 2007; 26:469–479. [PubMed: 17960325]
27. Kirsch M, Schackert G, Black PM. Metastasis and angiogenesis. Cancer treatment and research. 2004; 117:285–304. [PubMed: 15015566]
28. Kirsch M, Weigel P, Pinzer T, Carroll RS, Black PM, Schackert H-K, Schackert G. Therapy of hematogenous melanoma brain metastases with endostatin. Clinical cancer research: an official journal of the American Association for Cancer Res. 2005; 11:1259–1267.
29. Kripke ML. Latency, histology, and antigenicity of tumors induced by ultraviolet light in three inbred mouse strains. Cancer research. 1977; 37:1395–1400. [PubMed: 851959]
30. Lacy MQ, Jacobus S, Blood EA, Kay NE, Rajkumar SV, Greipp PR. Phase II study of interleukin-12 for treatment of plateau phase multiple myeloma (E1A96): a trial of the Eastern Cooperative Oncology Group. Leukemia research. 2009; 33:1485–1489. [PubMed: 19243818]

31. Lenzi R, Edwards R, June C, Seiden MV, Garcia ME, Rosenblum M, Freedman RS. Phase II study of intraperitoneal recombinant interleukin-12 (rhIL-12) in patients with peritoneal carcinomatosis (residual disease <1 cm) associated with ovarian cancer or primary peritoneal carcinoma. Journal of translational medicine. 2007; 5:66. [PubMed: 18076766]
32. Leon SP, Folkerth RD, Black PM. Microvessel density is a prognostic indicator for patients with astroglial brain tumors. Cancer. 1996; 77:362–372. [PubMed: 8625246]
33. MacDonald TJ, Taga T, Shimada H, Tabrizi P, Zlokovic BV, Cheresh DA, Laug WE. Preferential susceptibility of brain tumors to the antiangiogenic effects of an alpha(v) integrin antagonist. Neurosurgery. 2001; 48:151–157. [PubMed: 11152340]
34. Mitjans F, Meyer T, Fittschen C, Goodman S, Jonczyk A, Marshall JF, Reyes G, Piulats J. *In vivo* therapy of malignant melanoma by means of antagonists of alphav integrins. International journal of cancer Journal international du cancer. 2000; 87:716–723. [PubMed: 10925366]
35. Moran JP, Gerber SA, Martin CA, Frelinger JG, Lord EM. Transfection of the genes for interleukin-12 into the K1735 melanoma and the EMT6 mammary sarcoma murine cell lines reveals distinct mechanisms of antitumor activity. International journal of cancer Journal international du cancer. 2003; 106:690–698. [PubMed: 12866028]
36. Naumov GN, Bender E, Zurakowski D, Kang S-Y, Sampson D, Flynn E, Watnick RS, Straume O, Akslen LA, Folkman J, Almog N. A model of human tumor dormancy: an angiogenic switch from the nonangiogenic phenotype. Journal of the National Cancer Institute. 2006; 98:316–325. [PubMed: 16507828]
37. Naumov GN, Folkman J, Straume O. Tumor dormancy due to failure of angiogenesis: role of the microenvironment. Clinical & experimental metastasis. 2009; 26:51–60. [PubMed: 18563595]
38. Oliveira-Ferrer L, Hauschild J, Fiedler W, Bokemeyer C, Nippgen J, Celik I, Schuch G. Cilengitide induces cellular detachment and apoptosis in endothelial and glioma cells mediated by inhibition of FAK/src/AKT pathway. Journal of experimental & clinical cancer research: CR. 2008; 27:86. [PubMed: 19114005]
39. Onishi M, Ichikawa T, Kurozumi K, Date I. Angiogenesis and invasion in glioma. Brain tumor pathology. 2011; 28:13–24. [PubMed: 21221826]
40. Schackert G, Fidler IJ. Development of *in vivo* models for studies of brain metastasis. International journal of cancer Journal international du cancer. 1988; 41:589–594. [PubMed: 3356491]
41. Shi X, Cao S, Mitsuhashi M, Xiang Z, Ma X. Genome-wide analysis of molecular changes in IL-12-induced control of mammary carcinoma *via* IFN-gamma-independent mechanisms. Journal of immunology (Baltimore, Md: 1950). 2004; 172:4111–4122.
42. Taga T, Suzuki A, Gonzalez-Gomez I, Gilles FH, Stins M, Shimada H, Barsky L, Weinberg KI, Laug WE. alpha v-Integrin antagonist EMD 121974 induces apoptosis in brain tumor cells growing on vitronectin and tenascin. International journal of cancer Journal international du cancer. 2002; 98:690–697. [PubMed: 11920637]
43. Weis SM, Cheresh DA. Tumor angiogenesis: molecular pathways and therapeutic targets. Nature medicine. 2011; 17:1359–1370.
44. Xu M, Mizoguchi I, Morishima N, Chiba Y, Mizuguchi J, Yoshimoto T. Regulation of antitumor immune responses by the IL-12 family cytokines, IL-12, IL-23, and IL-27. Clinical & developmental immunology. 2010:2010.
45. Yamada S, Bu X-Y, Khankaldyyan V, Gonzales-Gomez I, McComb JG, Laug WE. Effect of the angiogenesis inhibitor Cilengitide (EMD 121974) on glioblastoma growth in nude mice. Neurosurgery. 2006; 59:1304–1312. discussion 1312. [PubMed: 17277694]
46. Yuzhalin AE, Kutikhin AG. Interleukin-12: clinical usage and molecular markers of cancer susceptibility. Growth factors (Chur, Switzerland). 2012; 30:176–191.

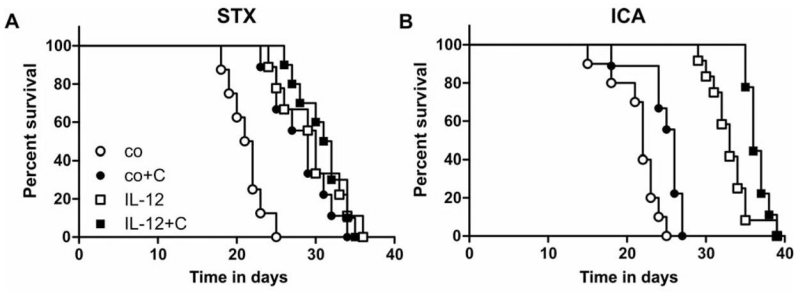

Figure 1.

Impact of anti-angiogenic therapies on survival time. Tumor cells (K1735) were either implanted by stereotactic injection into the brain (A) or by injection into the carotid artery to mimic hematogenic metastatic tumor formation (B). When the animals developed severe tumor signs and reached a defined endpoint they were euthanized. The graphs show the percentage of surviving animals over time. Animals without antiangiogenic therapy (wt: injection of K1735-wt cells: open circles) exhibited the shortest survival times. All therapies (wt+EMD: injection of K1735-wt cells with cilengitide therapy for 10 days, black circles; IL-12: injection of K1735-IL-12 cells, open squares; IL-12+EMD: injection of K1735-IL-12 cells with EMD121974 therapy for 10 days, black squares) resulted in prolonged survival ($p<0.0001$, Log-rank test for STX and ICA, n=8–12).

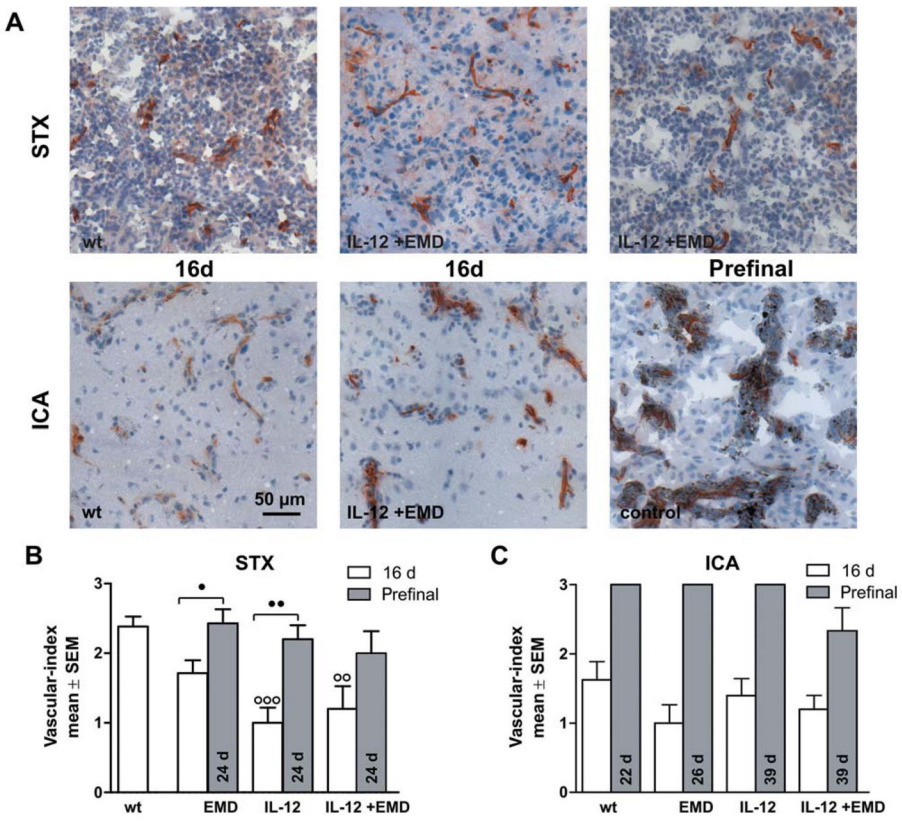

Figure 2.

Impact of anti-angiogenic therapies on microvessel phenotype. Brain tissue was investigated by CD31 immunohistochemistry. A: Representative pictures of brain sections (10-µm thick) stained with anti-CD31 after stereotactic injection of tumor cells (A, upper row, STX) and hematogenous metastases model (A, lower row, ICA) are shown. The experimental groups are indicated. Scale bar represents 50 µm. B, C: The vascular index was calculated as mean ±SD for the experimental groups after 16 days survival time (white) or at aprefinal stage (grey). Contralateral (normal) tissue always received a score of 0 (very fine, regular). B: After antiangiogenic treatment, there were more animals with finer blood vessels than in the untreated animals in the STX-model. At 16 days, an irregular architecture was found only in animals which had not been given treatment. After 24 d survival time, animals with a coarse and irregular network of microvessels were found in all groups investigated. C: In the ICA group, treatment had no effect on tumor-induced changes in microvessel morphology (score 0=very fine, regular, score 1=fine, regular, score 2=coarse, regular, score 3=coarse, irregular, ○○ and ○○○ difference versus wt group with $p<0.01$ and $p<0.001$, ● and ●● difference between treatment groups as indicated with $p<0.05$ and $p<0.01$, respectively. Same abbreviations as in Figure 1).

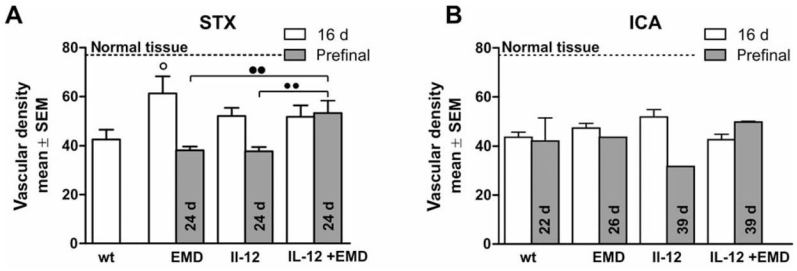

Figure 3.

Impact of anti-angiogenic therapies on microvessel density. The density of microvessels was investigated in brain sections by counting the number of CD31-positive structures/field using a 200-fold objective. The bars represent mean±SD for the experimental groups as indicated after 16 days survival time (white) and 24 days or long-surviving pre-final time (grey). Long term survival denotes those animals that were euthanized due to neurological or overall deterioration. The vascular density in normal tissue is indicated with a dashed line. A: Tumor formation led to the reduction of CD31-positive structures, and the antiangiogenic effectors partly prevented these changes at early stages after intracranial injection of melanoma cells. B: In metastases induced by intracarotoid injection of melanoma cells, the number of microvessels was markedly reduced. However, neither antiangiogenic therapies nor survival time influenced microvessel density (○ difference versus control group with $p<0.05$, ●● difference between treatment groups as indicated, $p<0.01$, respectively, same abbreviations as in Figure 1).

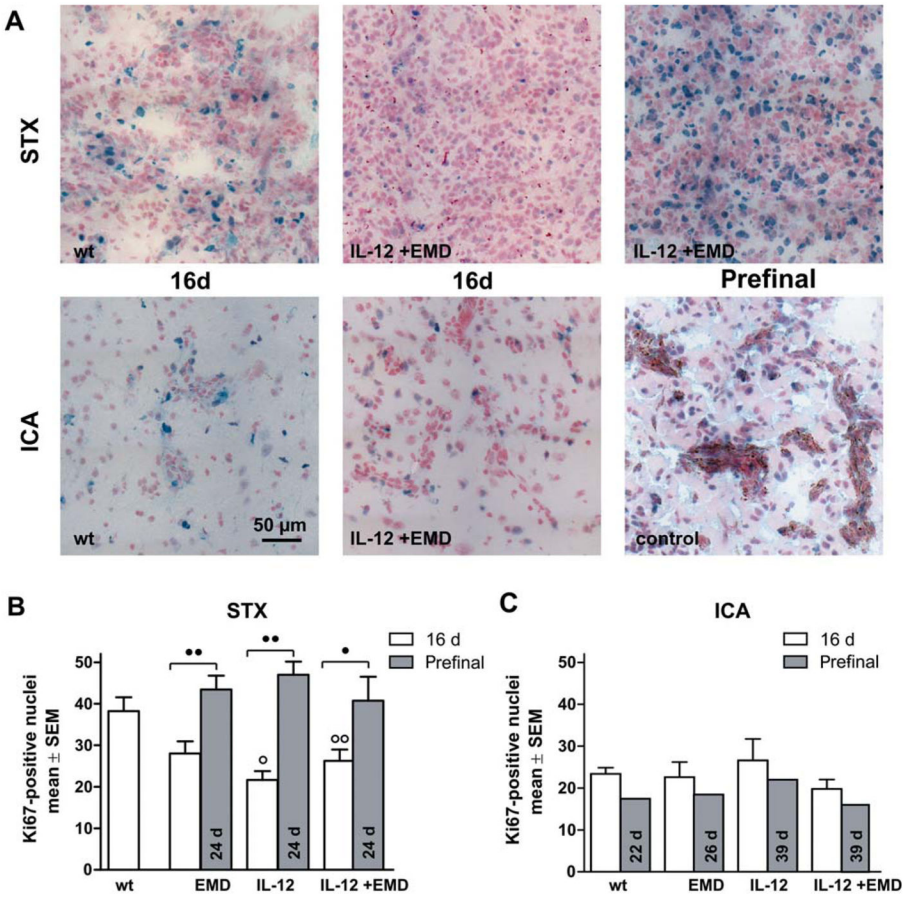

Figure 4.

Impact of anti-angiogenic therapy on proliferation. A: Representative pictures of brain sections (10-µm thick) stained with anti-Ki67 after stereotactic injection of tumor cells (A, upper row, STX) and hematogenous metastases model (A, lower row, ICA) are shown. The experimental groups were indicated. Scale bar represents 50 µm. B, C: The number of Ki67-positive nuclei in brain metastases was determined with a 200-fold objective. The bars represent mean ±SD for the experimental groups as indicated after 16 d survival time (white) or for long surviving prefinal animals (grey). B: In the STX model, antiangiogenic treatment transiently reduces proliferation at 16 day survival time compared to untreated animals but not at the prefinal survival time of 24 days. C: Ki67-positive nuclei were also detected in brain tissue in the hematogenous metastases model. In this model, we found comparable numbers of proliferating cells in all experimental groups, even after therapy or long term survival (○ and ○○ difference versus wt group with $p<0.05$ and $p<0.01$, ● and ●● difference between treatment groups as indicated with $p<0.05$ and $p<0.01$, respectively., same abbreviations as in Figure 1).